AN EXPERIMENTAL STUDY OF THE FLOW OF RAREFIED GAS AROUND A SPHERE

I. F. Zavarzina and I. V. Skokov

Zhurnal Prikladnoi Mekhaniki i Tekhnicheskoi Fiziki, Vol. 8, No. 2, pp. 93-96, 1967

The flow conditions for a low-density [rarefied] gas differ considerably from those for a continuous medium, as does the mechanism of interaction with a surface. In particular, the boundary layer and the shock wave become broader, and the aerodynamic and heat-transfer characteristics are thereby affected.

Of particular interest is the transition from a continuous medium to free-molecular flow. The methods of kinetic theory may be used to describe processes in low-density gases, but they are very complicated, so the Navier-Stokes equations are often used in conjunction with the equations for the boundary layer in the transition region, with boundary conditions that take into account the altered interaction. In particular, the Navier-Stokes equations predict a structure for a shock wave that agrees well with experiment [1].

Although there are several largely theoretical papers on the transition region [1-3], many aspects have not been elucidated, and this hinders consideration of the flow mechanism. There are very few experimental studies in this region, and these have employed mainly gasdynamic methods. One reason for this is the low state of development of optical methods for studying low-density flows.

Interferometry is the most widely used method of examining gasdynamic processes in a continuous medium. Since a low-density gas flowing around a model produces only a very small density change, the recording of phase shifts requires interference systems of high sensitivity such as a multiple-beam interferometer, in which the beam passes repeatedly through the object and so provides higher sensitivity than does a single transit [5, 6].

Figure 1 shows the apparatus. The multiple-beam interferometer consists of two plane-parallel plates 5 bearing semitransparent multilayer dielectric coatings (reflectivity A = 85%). Light source 1 (low-pressure mercury lamp) works into filter 2 and lens 3, which together produce a collimated beam of monochromatic light. The interference pattern is recorded with the optical system consisting of lens 8, stop 9, and camera 10. The gas jet from nozzle 6 passes between the mirrors and falls on model 7. The chamber is fitted with protective glass windows 4.

The instrument is used and the patterns are processed as previously described [6]. A notable feature is the use of remote control of the interferometer plates, together with the inverse piezoelectric effect for fine adjustment [7], in which one varies the voltage applied to three barium titanate ceramic spacers attached to one of the mirrors. After the plates have been set parallel (e. g., via equal-inclination fringes), stop 9 is set in the focal plane of lens 8 to isolate the central part of the fringe system, which is then seen as a uniformly illuminated area. The sensitivity is substantially dependent on the illumination level relative to the maximum [8], so the control voltage is adjusted to the optimum setting, i. e., the one giving maximum contrast.

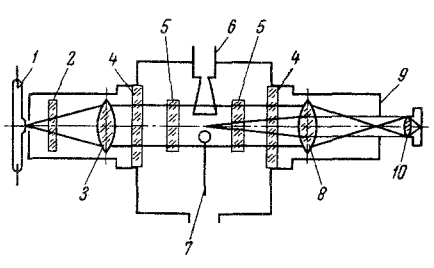

Fig. 1

The patterns are interpreted by means of the differences in density corresponding to the incident flow (D_∞) and the shock layer (D_s). This method has [6] been applied to two-dimensional flows. Here our technique was adapted to the axial symmetry of the flow.

The increment in the density ρ at a point in the field relative to the density ρ_∞ of the unperturbed flow is [6, 9, 10] given by

$$\rho - \rho_\infty = \frac{\lambda}{\pi K \xi y^*} \frac{d}{dy^*} \int_{r_i}^{1} \frac{(D_s - D_\infty)\, r^* dr^*}{\sqrt{r^{*2} - r_i^{*2}}},$$

$$r_i^* = y / r^\circ, \qquad r^* = r / r^\circ,$$

in which λ is the wavelength of the light, K is Gladstone's constant, y is the coordinate along the beam in the flow (the y-axis lies in a plane normal to the axis of the flow), r° is the radius of the axially symmetric flow, and r is the radial coordinate for the beam in the flow.

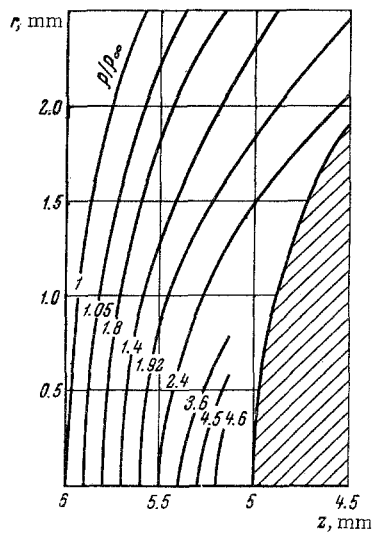

Fig. 2

The quantity ξ is [6, 8-10] expressed as

$$\xi = \frac{16\pi\gamma}{2.3} \frac{[2.3A(D_{\max} - D_\infty)/\gamma]^{1/2}}{[1 + 2.3(D_{\max} - D_\infty)/\gamma](1 - A)},$$

in which γ is the contrast factor of the photographic material and Dmax is the density at the peak of an interference fringe.

The cross section of the axially symmetric inhomogeneity is divided into N = 5 annuli, in each of which the density difference is represented by a polynomial of second degree by means of the observed densities at the edges and center. The density increment is

$$\rho_i - \rho_\infty = \sum_{j=i-1}^{2N-1} \alpha_{j,i} [D(r_j) - D_\infty],$$

in which r_j is the radius of zone j and α is a constant which can be calculated [9, 10]. We have examined the flow around a sphere of radius 5 mm at Mach numbers M of 3.85-4.02 and Reynolds numbers (calculated from the flow parameters) R of 75-230.

Figure 2 shows the observed result for the density distribution in front of the sphere for M_∞ = 4.02 and R = 230, the ordinate being the distance r from the axis and the abscissa being the axial coordinate z, the origin lying at the center of the sphere. The curves are lines of equal ρ/ρ_∞. Figures 3 and 4 show density profiles for the shock wave near the front critical point of the sphere at R of 75 and 230 respectively. The observed ρ/ρ_∞ for various z are as follows:

$z =$	5.25	5.45	5.75	5.95	(for $R = 75$)
$\rho/\rho_\infty =$	4.6	3.5	1.2	1.05	

$z = 5.35$	5.55	5.65	5.75	(for $R = 230$)
$\rho/\rho_\infty = 4.3$	2.3	1.8	1.45	

Curves 2 in Figs. 3 and 4 are from [11] and represent the profile of the shock wave calculated as a function of M and the mean free

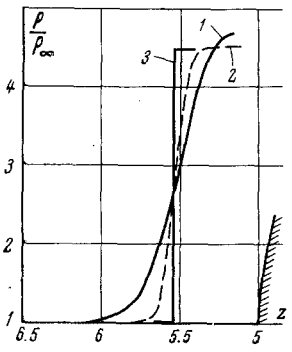

Fig. 3

path in the incident flow. Curves 3 are for a continuum [4] and allow one to estimate the distance to the shock wave and ρ/ρ_∞. The observed curves 1 and Mott-Smith curves 2 have been placed to bring the inflection on the latter at the point z^* on the experimental curve with the same ordinate [12,13]. The curves show that the shock wave is broad (~8-10 mean free paths) in the range of R used. These results are somewhat larger than those previously given [1,2,12,13]. The difference arises because we have taken as the thickness of the shock wave the value z^* at which ρ differs from the density in the incident flow and behind the step by roughly 5%. For R = 230 there is a fairly broad region in which the density in the shock layer is virtually unaltered; the density behind the step takes virtually the continuum value calculated from Hugoniot's relations. The thickness is greater at R = 75, and Hugoniot's relations continue to apply, but there is no obvious zone of constant density. In this case there is no separate zone of nonviscous flow. The boundary layer and shock wave begin to meet.

Both modes have gradual density change in the shock wave, slower on the incident side.

The separation of the shock has [12,13] been taken as the distance from the body to point z^*, but we consider it more correct to take the start as the zone where ρ/ρ_∞ starts to differ from unity, e.g., by 5%. The separations Δ° measured in this way for various R are shown by curve 1 in Fig. 5, where curve 2 represents the results given by the

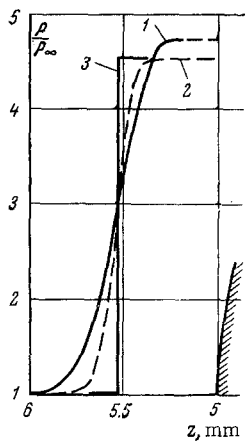

Fig. 4

Navier-Stokes equations for a viscous shock layer in flow around a thermally insulated body. The Δ° for the various R are as follows:

$R = 100$	200	400	600	700
$\Delta^\circ = 0.179$	0.172	0.160	0.154	0.152 (calc.)
$\Delta^\circ = 0.171$	0.162	0.141	0.124	0.121 (exp.)

It has been assumed in the solution that a thin shock wave is formed around the sphere, whose shape is nearly spherical in the region of the critical point. The entire space between the shock wave and the body is occupied by a viscous layer. As external boundary conditions we took Hugoniot's relations at the step, on the assumption of absence of slip and of a heat flux from the surface. As the discussion was restricted to the region of the critical point, there was local similarity [3]. The numerical integration was performed for M_∞ = = 5, $\varkappa = c_p/c_v = 1.4$, and P = 0.72 for R of 100-1000.

Figure 5 shows that the thickness of the shock layer falls as the density increases, and the shock wave approaches the body. The discrepancy between the theoretical and experimental curves increases somewhat with R. The smaller discrepancy for small R may be ascribed to the completely viscous dissipative layer behind the step (Fig. 3), but the shock wave is diffuse in the range examined, which conflicts with the viscous-layer model used. On the other hand, the Hugoniot relations at the step are obeyed (within the error of experiment) before the gas flow reaches the body. This explains the reasonably satisfactory agreement between the observed and calculated curves in Fig. 5.

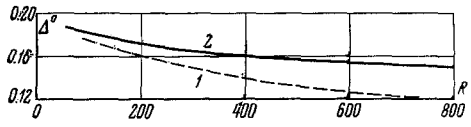

Fig. 5

Our results and conclusions agree well with Ivanov's [12,13]; he examined the flow around a sphere at M_∞ = 6 and R_∞ = 200 by means of an electron beam.

REFERENCES

1. F. S. Sherman and L. Talbot, Rarefied Gasdynamics, edited by F. M. Devienne, ILL, 266-311, 1963.

2. W. D. Hayes and R. F. Probstein, Hypersonic Flow Theory, Izd. inostr. lit., 1962.

3. R. F. Probstein and N. H. Kemp, "Viscous aerodynamic characteristics in hypersonic rarefied gas flow," J. Aerospace Sci., vol. 27, no. 3, 174-192, 1960.

4. W. Chester, "Supersonic flow past a bluff body with a detached shock. Part II, Axisymmetrical body," J. Fluid Mech., vol. 1, no. 5, 490-496, 1956.

5. F. A. Korolev, G. I. Kromskii, and I. V. Skokov, "Use of the phase method in multiple-beam interferometry of measuring low gas densities," Izv. VUZ. Fizika, no. 5, 61, 1963.

6. F. A. Korolev, A. I. Akimov, G. I. Kromskii, and I. V. Skokov, "Use of a Fabry-Perot etalon for studying low-density air flows," Pribory i tekh. eksp., no. 4, 243, 1965.

7. D. J. Bradley, "Parallel movement for high-finesse interferometer scanning," J. Sci. Instr., vol. 39, no. 2, 41, 1962.

8. I. V. Skokov, "Comparison of double-beam and multiple-beam interferometers for sensitivity in measuring small variations in the refractive index," Vestnik Mosk. Univ., no. 2, 82, 1962.

9. V. A. Emel'yanov, "Interferometric study of gas inhomogeneities with a stepped density distribution," Inzh.-fiz. zh., no. 1, 1963.

10. V. A. Emel'yanov and G. P. Zhavrid, "Numerical solution of problems arising in optical studies of axially symmetric inhomogeneities," Inzh.-fiz. zh., no. 4, 1962.

11. H. M. Mott-Smith, "Solution of the Boltzmann equation for a shock wave," Phys. Rev., vol. 82, no. 6, 885, 1951.

12. A. V. Ivanov, "Density near the critical point of a blunt body in a supersonic flow of rarefied gas," Dokl. AN SSSR, **161**, 315, 1965.

13. A. V. Ivanov, "Determination of the density ahead of a blunt body in a supersonic flow of rarefied gas," PMTF, 6, 99, 1964.

27 August 1966 Moscow